24 Sep 2013

Dynamic Nonlinearity and Nonlinear Single-Degree-Of-Freedom Model for Cable Net Glazing

Ruo Qiang Feng

Jihong Ye

Guirong Yan
Missouri University of Science and Technology, yang@mst.edu

Jin Ming Ge

Recommended Citation

R. Q. Feng et al., "Dynamic Nonlinearity and Nonlinear Single-Degree-Of-Freedom Model for Cable Net Glazing," *Journal of Engineering Mechanics*, vol. 139, no. 10, pp. 1446 - 1459, American Society of Civil Engineers, Sep 2013.
The definitive version is available at https://doi.org/10.1061/(ASCE)EM.1943-7889.0000575

Dynamic Nonlinearity and Nonlinear Single-Degree-of-Freedom Model for Cable Net Glazing

Ruo-Qiang Feng, M.ASCE[1]; Jihong Ye[2]; Guirong Yan[3]; and Jin-Ming Ge[4]

Abstract: The nonlinear vibration differential equation and vibration frequency of cable net glazing subject to earthquake loading was determined, and a geometrically nonlinear single-degree-of-freedom model for cable net glazing was developed. The nonlinear response spectra were established, and nonlinear time history analysis with finite element (FE) models was conducted to verify them. The nonlinear vibration differential equation and frequency obtained as described in this paper provide a basis for the nonlinear single-degree-of-freedom model for cable net glazing. The analytical formula for the nonlinear frequency with a simplified expression is highly precise and convenient for use in engineering practice. For larger-amplitude seismic waves, the difference between the linear and nonlinear response spectra are more obvious. As the natural period of cable net glazing is always less than 2 s, the linear response spectra in the Chinese code for the seismic design of buildings can be used in the seismic design of cable net glazing as an approximation rather than the nonlinear response spectra of cable net glazing.
DOI: 10.1061/(ASCE)EM.1943-7889.0000575.

CE Database subject headings: Cables; Seismic design; Vibration; Earthquake loads; Coating.

Author keywords: Point-supported glazing system; Geometric nonlinearity; Cable structure; Response spectra; Seismic design.

Introduction

Cable net glazing is becoming increasingly appealing because of its translucence, lightness, and energy savings. It is attractive from both an architectural and a climatic point of view, as shown in Fig. 1. The earliest research in the design of cable net glazing was conducted by Schlaich (2004), Schlaich et al. (2005), Schober and Scheider (2004), and Feng et al. (2009). Those designs are widely used in airport passenger terminals, exhibition centers, gymnasia, and hotel halls.

The technological and morphological aspects of the connection joints of cable net glazing were first addressed by Vyzantiadou and Avdelas (2004). The construction details of the point-fixed connection joints were analyzed by Brodniansky and Aroch (2001) and by Saitoh et al. (2001). The mechanical behavior of the glass panels was studied by Feng et al. (2007, 2012). Feng et al. (2007, 2009) investigated the effect of the stiffness of the glass panels on the static and dynamic performance of cable net glazing. A shaking table test of cable net glazing was conducted by Feng et al. (2010) to investigate the connection between cable and glass panels in earthquakes.

However, very little research has been conducted on the geometric nonlinearity and nonlinear seismic performance of cable net glazing. While cable net glazing is a structurally important part of a building, the loss of glass panels because of seismic activity cannot be neglected. In the Michoacán, Mexico, earthquake in 1985, according to the disaster statistics, 63 of the 263 total glass panels were broken. In the Northridge, California, earthquake in 1994, 40–60% of glass panels were broken (Pantelides et al. 1996). In addition to the direct losses caused by the earthquake, secondary losses included injuries and deaths caused by the fallen glass panels.

Cable net glazing is a plane structure that does not have a negative Gauss curvature and thus has a relatively lower stiffness in the direction perpendicular to the plane of the cable net. The permissible deflection of cable net glazing is normally 1/50 of the span, but for some special cases, it may be 1/40 of the span in technical specification for cable structures of China JGJ257–2012 (Ministry of Construction 2012), which indicates that it is important to consider geometric nonlinearity in the analysis of cable net glazing. The frequencies of a cable net depend on its displacement. The vibrating displacement of a cable net changes when it is subjected to seismic loads, and the frequencies of the cable net also change (Feng et al. 2009). The response spectrum method in the seismic design code (Ministry of Construction 2010) of China for linear and elastic structures thus has some limitations with respect to the seismic design of nonlinear cable net glazing, and the geometric nonlinear response spectra for cable net glazing must be studied. In the Chinese technical code for glass curtain wall engineering by Ministry of Construction (2003) of China, the seismic force on glass panels is five times the maximum seismic force on buildings, but this seismic design method for glass panels is not applicable to cable net glazing, and it greatly increases the seismic force on cable net glazing (Ministry of Construction 2010).

In this study, the nonlinear static equilibrium equation and the nonlinear vibration differential equation of cable net glazing subject to dynamic loads were determined, and the static and dynamic

[1]Associate Professor, School of Civil Engineering, Key Laboratory of Concrete and Prestressed Concrete Structures of Ministry of Education, Southeast Univ., Nanjing 210096, China; presently, Visiting Associate Professor, State Key Laboratory of Subtropical Building Science, South China Univ. of Technology, Guangzhou 510500, China (corresponding author). E-mail: hitfeng@163.com

[2]Professor, School of Civil Engineering, Key Laboratory of Concrete and Prestressed Concrete Structures of Ministry of Education, Southeast Univ., Nanjing 210096, China. E-mail: yejihong@seu.edu.cn

[3]Assistant Professor, Dept. of Civil Engineering, Univ. of Texas, El Paso, TX 79902. E-mail: gyan@utep.edu

[4]Master Student, Department of Civil Engineering, School of Civil Engineering, Key Laboratory of Concrete and Prestressed Concrete Structures of Ministry of Education, Southeast Univ., Nanjing 210096, China.

Note. This manuscript was submitted on April 13, 2011; approved on November 29, 2012; published online on April 3, 2013. Discussion period open until March 1, 2014; separate discussions must be submitted for individual papers. This paper is part of the ***Journal of Engineering Mechanics***, Vol. 139, No. 10, October 1, 2013. ©ASCE, ISSN 0733-9399/2013/10-1446–1459/$25.00.

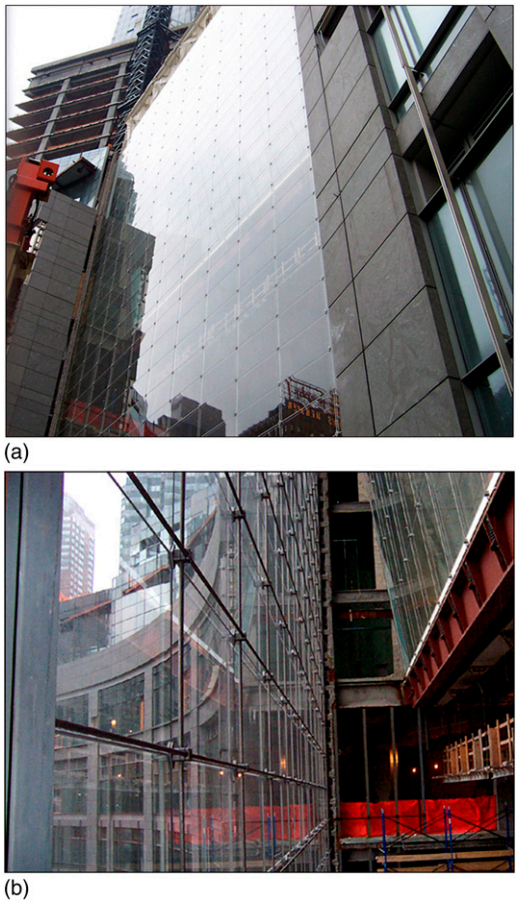

Fig. 1. Time Warner Center in New York; (a) outside view; (b) inside view

geometric nonlinearity of cable net glazing was examined. A geometrically nonlinear single-degree-of-freedom model for cable net glazing was developed, and a nonlinear time history analysis was conducted with an FE model to verify the nonlinear single-degree-of-freedom model. The nonlinear single-degree-of-freedom model was then used to determine the nonlinear seismic response of cable net glazing subject to seismic waves with the time history method. The linear and nonlinear acceleration and displacement spectra were compared. Finally, on the basis of nonlinear spectra, the seismic response of cable net glazing was analyzed by the mode decomposition response spectra method.

Nonlinear Static Equilibrium Equation of Cable Net Glazing Based on Membrane Theory

Membrane theory by Krishna (1978) is adopted to determine the nonlinear static equilibrium equation of a cable net, and the cable net is modeled in the form of an isotropic continuous membrane. The analytical expressions of the nonlinear static equilibrium equation can be obtained with good precision using membrane theory by Irivne (1992).

The assumptions in this paper are as follows:

1. The cable net is assumed to be a continuous isotropic tension-only membrane,
2. Only the out-of-plane nodal displacements of the cable net are considered, and the in-plane nodal displacements are neglected, and

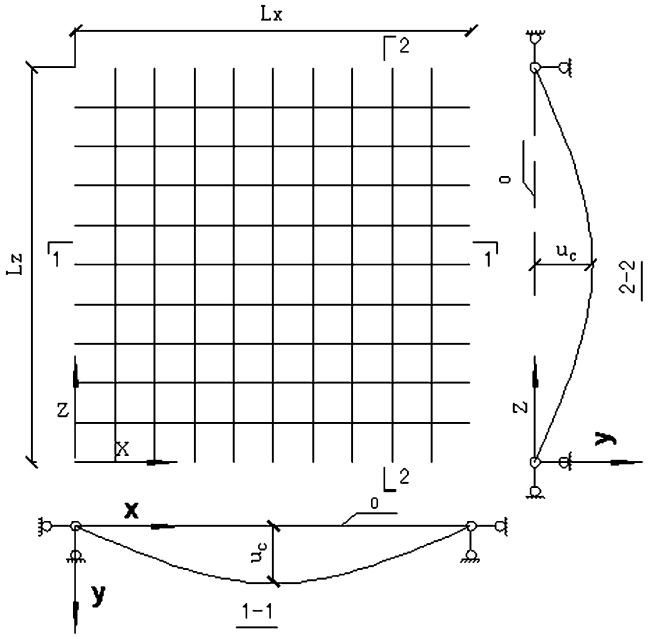

Fig. 2. Model of a cable net facade

3. The displacement shape of the cable net subject to uniformly distributed loads is assumed to be a symmetric function, namely $\varphi_1(x,y) = \sin[\pi(x/L_x)]\sin[\pi(z/L_z)]$.

where the coordinate system is shown in Fig. 2, the horizontal direction is assumed to be the x direction, the wind direction is the y direction, the vertical direction is the z direction, and the origin of the coordinates is the left corner of the cable net glazing.

When the central nodal displacement of the structure is u_c, any nodal displacement is

$$u = u_c \sin\left[\pi\left(\frac{x}{L_x}\right)\right]\sin\left[\pi\left(\frac{z}{L_z}\right)\right] \tag{1}$$

Subject to uniformly distributed loads, the static equilibrium equation of any node in the cable net is

$$\left(\overline{H_x} + \overline{h_x}\right)\frac{\partial^2 u}{\partial x^2} + \left(\overline{H_z} + \overline{h_z}\right)\frac{\partial^2 u}{\partial z^2} = -P_0 \tag{2}$$

where $\overline{H_x}$ and $\overline{H_z}$ = unit-distance horizontal components of the initial cable pretension in the x and z directions, $\overline{h_x}$ and $\overline{h_z}$ = unit-distance horizontal components of the cable tension increment in the x and z directions, and P_0 = uniform-distributed load.

The expressions for $\overline{h_x}$ and $\overline{h_z}$ are

$$\overline{h_x} = E\overline{A_x}\Delta L_x / L_x \tag{3}$$

$$\overline{h_z} = E\overline{A_z}\Delta L_z / L_z \tag{4}$$

where $\overline{A_x}$ and $\overline{A_z}$ = unit-distance cross-sectional areas of the cables in the x and z directions, and E = Young's modulus of the cable.

The elongation of the cable is

$$\Delta L_x = \frac{1}{2}\int_0^{Lx}\left(\frac{\partial y}{\partial x}\right)^2 dx = u_c^2 \sin^2\left(\frac{\pi z}{L_z}\right)\Big/(4L_x) \tag{5}$$

J. Eng. Mech., 2013, 139(10): 1446-1459

$$\Delta L_z = \frac{1}{2}\int_0^{Lz}\left(\frac{\partial y}{\partial z}\right)^2 dz = u_c^2 \sin^2\left(\frac{\pi x}{L_x}\right)\Big/(4L_z) \tag{6}$$

By substitution of Eqs. (3)–(6) into Eq. (1), one obtains

$$\overline{H_x}\frac{\partial^2 u}{\partial x^2} + \overline{H_z}\frac{\partial^2 u}{\partial z^2} + EA_x\frac{\pi^2 u_c^2}{4L_x^2}\sin^2\left(\frac{\pi z}{L_z}\right)\frac{\partial^2 u}{\partial x^2} + EA_z\frac{\pi^2 u_c^2}{4L_z^2}\sin^2\left(\frac{\pi x}{L_x}\right)\frac{\partial^2 u}{\partial z^2} = -P_0 \tag{7}$$

Eq. (7) is the nodal displacement in the cable net. When the left and right sides of Eq. (7) are integrated in the field of integration of the whole cable net, the structural equilibrium equation of the cable net can be obtained after simplification as

$$\left(\frac{\overline{H_x}}{L_x^2} + \frac{\overline{H_z}}{L_z^2}\right)u_c + \left(EA_x\frac{\pi^2}{6L_x^4} + EA_z\frac{\pi^2}{6L_z^4}\right)u_c^3 = \frac{P_0}{4} \tag{8}$$

where the linear part of the structural stiffness is

$$a = \left(\frac{\overline{H_x}}{L_x^2} + \frac{\overline{H_z}}{L_z^2}\right) \tag{9}$$

and the nonlinear part of the structural stiffness is

$$b = \left(EA_x\frac{\pi^2}{6L_x^4} + EA_z\frac{\pi^2}{6L_z^4}\right)u_c^2 \tag{10}$$

When the structural span is determined, Eq. (9) shows that the initial linear part of the structural stiffness of the cable net is decided only by the cable pretension. Eq. (10) shows that the nonlinear part of the structural stiffness is decided by the cable axial rigidity and structural displacement, and it also shows that cable net glazing is a stiffness-hardening structure. The nonlinear coefficient λ is defined as the ratio between the nonlinear part and the linear part of the structural stiffness, and the expressions for λ is

$$\lambda = \frac{b}{a} = \frac{\left[EA_x\left(\pi^2/6L_x^4\right) + EA_z\left(\pi^2/6L_z^4\right)\right]u_c^2}{\overline{H_x}/L_x^2 + \overline{H_z}/L_z^2} \tag{11}$$

Example 1 is presented to illustrate the role of the nonlinear coefficient λ. The analysis model is shown in Fig. 2. The size of the model is 15×15 m with the glass mesh being 1.5×1.5 m, and the concentrated nodal mass is 146.25 kg (for a thickness of midhollow armored glass of 8 mm + 8 Air mm + 8 mm). The cable pretensions $\overline{H_x}$ and $\overline{H_z}$ are 20 kN, the areas of the cables in the x and z directions are 202.3E − 6 m^2, and the Young's modulus of the cables is 1.3E11 N/m^2. The maximum central nodal displacement under the action of mean wind load is $1/150$ of the span of the cable net.

As the cable axial rigidity and structural displacement increase, the nonlinear coefficient λ increased. Assuming that $A_x = A_z$ and $L_x = L_z$, the initial cable strain is $\alpha = H_x/EA_x$. Eq. (11) can be further simplified as

$$\lambda = \frac{\pi^2 u_c^2}{6\alpha L_x^2} \tag{12}$$

As shown in Eq. (12), the nonlinear coefficient λ is decided by the initial strain α and the square of the dimensionless deformation u_c/L_x. The curve of the nonlinear coefficient λ and the dimensionless deformation u_c/L_x with three types of initial cable strain are shown in Fig. 2. As shown in Fig. 3, when the dimensionless displacement is less than or equal to 1/250, the nonlinear coefficient λ is less than 3%; when the dimensionless displacement is 1/50, the nonlinear coefficient is more than 26%. These results demonstrate that the nonlinear part of the structural stiffness plays an important role and should be considered.

Nonlinear Vibration Differential Equation of Cable Net Glazing Based on Membrane Theory

Membrane theory by Krishna (1978) is also employed to determine the nonlinear vibration equation of a cable net subject to seismic loading.

The assumptions are as follows:

Assumptions 1 and 2 are the same as in Nonlinear Static Equilibrium Equation of Cable Net Glazing Based on Membrane Theory:

3. The first mode makes the dominant contribution to the seismic response of a cable net subject to seismic loading in the usual range of height–width ratios (0.5–2) by Feng et al. (2009, 2010),
4. The first mode is assumed to be a symmetric function, namely, $\varphi_1(x,z) = \sin[\pi(x/L_x)]\sin[\pi(z/L_z)]$.

As the first mode makes the dominant contribution to the seismic response, the central nodal displacement of the structure is $w(t)$, and any nodal vibrating displacement is

$$w_1(x,z,t) = w(t)\sin\left(\pi\frac{x}{L_x}\right)\sin\left(\pi\frac{z}{L_z}\right) \tag{13}$$

Subject to seismic loads, any nodal displacement vibration equation of the cable net can be derived from Newton's second law by Krishna (1978)

$$m\frac{\partial^2 w_1}{\partial t^2} - \left(\overline{H_x}\frac{\partial^2 w_1}{\partial x^2} + \overline{H_z}\frac{\partial^2 w_1}{\partial z^2} + \overline{h_x}\frac{\partial^2 w_1}{\partial x^2} + \overline{h_z}\frac{\partial^2 w_1}{\partial z^2}\right) + c\frac{\partial w_1}{\partial t} = m\ddot{w}_g(t) \tag{14}$$

where $\ddot{w}_g(t)$ is ground motion acceleration.

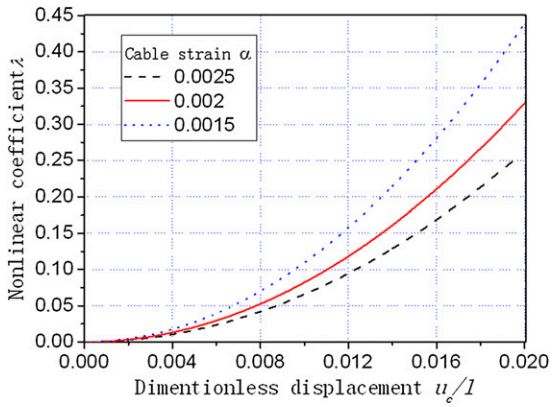

Fig. 3. Curve of λ versus dimensionless displacement for different initial cable strains

J. Eng. Mech., 2013, 139(10): 1446-1459

The elongation of the cable is

$$\Delta L_x = \frac{1}{2}\int_0^{Lx}\left(\frac{\partial w_1}{\partial x}\right)^2 dx \tag{15}$$

$$\Delta L_z = \frac{1}{2}\int_0^{Lz}\left(\frac{\partial w_1}{\partial z}\right)^2 dz \tag{16}$$

After substitution of Eqs. (13), (15), and (16) into Eqs. (3) and (4), the cable tension increment is

$$\overline{h_x} = \pi^2 E\overline{A_x} w(t)^2 \sin^2\left(\frac{\pi z}{L_z}\right)\Big/\left(4L_x^2\right) \tag{17}$$

$$\overline{h_z} = \pi^2 E\overline{A_z} w(t)^2 \sin^2\left(\frac{\pi x}{L_x}\right)\Big/\left(4L_z^2\right) \tag{18}$$

By substitution of Eqs. (17) and (18) into Eq. (14), one obtains

$$m\frac{\partial^2 w_1}{\partial t^2} - \left[\overline{H_x} + \pi^2 E\overline{A_x}\frac{w(t)^2}{4L_x^2}\sin^2\left(\frac{\pi z}{L_z}\right)\right]\frac{\partial^2 w_1}{\partial x^2} - \left[\overline{H_z} + \frac{\pi^2 E\overline{A_z} w(t)^2}{4L_z^2}\sin^2\left(\frac{\pi x}{L_x}\right)\right]\frac{\partial^2 w_1}{\partial z^2} + c\frac{\partial w_1}{\partial t} = m\ddot{w}_g(t) \tag{19}$$

where m is the mass of a unit area of the cable net and c is the damping.

Eq. (19) is the nodal displacement vibration equation in the cable net. When the left and right sides of Eq. (19) are integrated in the field of integration of the whole cable net, the structural displacement vibration equation of the cable net can be obtained as follows after simplification:

$$m\ddot{w}(t) + c\dot{w}(t) + \left[\frac{\pi^2\overline{H_x}}{L_x^2} + \frac{\pi^2\overline{H_y}}{L_y^2} + \frac{2}{3}\left(\frac{\pi^2}{L_x^2}\frac{\pi^2 EA_x}{4L_x^2} + \frac{\pi^2}{L_z^2}\frac{\pi^2 EA_z}{4L_z^2}\right)w^2(t)\right]w(t) = \int_0^{L_x}\int_0^{L_z}\frac{m\ddot{w}_g(t)dx\,dz\pi^2}{4L_xL_z} \tag{20}$$

Eq. (20) is the nonlinear vibration differential equation of the cable net subject to seismic loading. The linear part of the structural stiffness is $[(\pi^2\overline{H_x}/L_x^2) + (\pi^2\overline{H_z}/L_z^2)]$, while the nonlinear part is $2/3[(\pi^2/L_x^2)(\pi^2 EA_x/4L_x^2) + (\pi^2/L_z^2)(\pi^2 EA_z/4L_z^2)]w^2(t)$, and the structural vibrating displacement $w(t)$ is included.

Eq. (20) can be further simplified as

$$m\ddot{w}(t) + c\dot{w}(t) + (k_l + k_n)w(t) = \int_0^{L_x}\int_0^{L_z}\frac{m\ddot{w}_g(t)dx\,dz\pi^2}{4L_xL_z} \tag{21}$$

where $k_l = (\pi^2\overline{H_x}/L_x^2 + \pi^2\overline{H_z}/L_z^2)$ is the linear part of the structural stiffness in the vertical position and $k_n = 2/3[(\pi^2/L_x^2)(\pi^2 EA_x/4L_x^2) + (\pi^2/L_z^2)(\pi^2 EA_z/4L_z^2)]w^2(t)$ is the nonlinear part of the structural stiffness.

In the preceding nonlinear differential equation, Eq. (21), the square nonlinearity is included, so Eq. (21) is the Duffing equation. Given that $b > 0$ and that Eq. (21) is the hard-spring type of the Duffing equation, the corresponding mathematical method is used to solve the nonlinear frequency.

Derivation of the Analytic Formula of the Nonlinear Frequency

The free vibration equation without damping of Eq. (21) is

$$\ddot{w}(t) + aw(t) + bw^3(t) = 0 \tag{22}$$

where $a = (\pi^2\overline{H_x}/L_x^2 + \pi^2\overline{H_y}/L_y^2)/m, b = 2/3[(\pi^2/L_x^2)(\pi^2 EA_x/4L_x^2) + (\pi^2/L_z^2)(\pi^2 EA_z/4L_z^2)]/m$.

The structural stiffness is $k = [a + bw^2(t)]m$, and the linear structure's frequency ω_L is

$$\omega_L^2 = k_1/m = a \tag{23}$$

where the structural stiffness k is nonlinear and includes the structural displacement $w(t)$. It is obvious that the structural frequency cannot be calculated by Eq. (23) and that the frequency must be obtained by directly solving the nonlinear vibration differential equation.

Integral Algorithm of Nonlinear Frequency

The structural acceleration $\ddot{w}$ can be changed as follows by Nayfeh and Mook (1979) and Dechao and Yufeng (2004)

$$\ddot{w} = \frac{d\dot{w}}{dt} = \frac{d\dot{w}}{dw}\frac{dw}{dt} = \frac{d\dot{w}}{dw}\dot{w} = \frac{1}{2}\frac{d(\dot{w})^2}{dw} \tag{24}$$

So Eq. (24) can be written as

$$\frac{1}{2}\frac{d(\dot{w})^2}{dw} + aw + bw^3 = 0 \tag{25}$$

Because the structural velocity in the amplitude position is zero, integrating Eq. (25) yields

$$\frac{1}{2}\dot{w}^2 = \int_w^A (aw + bw^3)dw \tag{26}$$

where A is the amplitude.

According to Eq. (26), one can obtain the expression of the velocity in any position

$$\dot{w} = \frac{dw}{dt} = \sqrt{2\int_w^A (aw + bw^3)dw} \tag{27}$$

Eq. (27) can be written as

$$dt = \frac{dw}{\sqrt{2\int_w^A (aw + bw^3)dw}} \tag{28}$$

Thus the structural vibration period is

J. Eng. Mech., 2013, 139(10): 1446-1459

$$T = \int_0^T dt = 4\int_0^A \frac{dw}{\sqrt{2\int_w^A (aw + bw^3)dw}} \tag{29}$$

Eq. (29) can be simplified as

$$T = 4\int_0^A \frac{dw}{\sqrt{a(A^2 - w^2) + \frac{b}{2}(A^4 - w^4)}} \tag{30}$$

Eq. (30) is the accurate integral algorithm of the nonlinear frequency $\omega = 2\pi/T$, but it cannot be simplified continuously. It can be solved only by the numerical method, which is not convenient for use. Therefore, the harmonic balance method is used to determine the simplified expression of the nonlinear frequency, which fits well in a strongly nonlinear system by Dechao and Yufeng (2004).

Harmonic Balance Method

Because there are cubic nonlinear parts in the nonlinear differential equation, the assumed displacement solution should include the first-order harmonic components and constant

$$w = A\cos\omega t \tag{31}$$

Substitution of Eq. (31) into Eq. (22) yields

$$\left(a + \frac{3bA^2}{4} - \omega^2\right)A\cos\omega t + \frac{bA^3\cos 3\omega t}{4} = 0 \tag{32}$$

When $\cos 3\omega t$ is neglected and only $\cos\ \omega t$ is considered, the analytic formula for the structural nonlinear frequency can be obtained

$$\omega = \omega_L\sqrt{1 + \frac{3b}{4a}A^2} = \omega_L(e + 1) \tag{33}$$

where ω_L is the linear frequency of the structure. The coefficient of the nonlinear frequency e is

$$e = \sqrt{1 + \frac{3b}{4a}A^2} - 1 \tag{34}$$

The structural amplitude is included in Eq. (34), and the coefficient of the nonlinear frequency e displays the effect of the geometric nonlinearity on the nonlinear frequency.

Curves of the coefficient e versus the ratio of the amplitude to the span for three types of cable strain are shown in Fig. 4. When the amplitude is less than 1/250 of the span, the coefficient of the nonlinear frequency is negligible. The coefficient e increases at an increasing rate as the structural amplitude increases. When the amplitude is 1/50 of the span, the coefficient is less than 16%, and the dynamic geometric nonlinearity is less than the static geometric nonlinearity.

Verification of the Analytic Formula of the Nonlinear Frequency

To verify the accuracy of the analytical formula for the nonlinear frequency given by Eq. (33), the nonlinear frequency results obtained from the integral algorithm method [Eq. (30)], the analytic formula [Eq. (33)], and the nonlinear FEM time history method are compared. In the nonlinear FEM time history method, the initial displacement with a known amplitude is applied to the cable net, and then the cable net vibrates freely without damping. Thus the nonlinear frequency can be calculated directly from the time history displacement curve.

The analysis model is shown in Fig. 2. The size of the model is 15×15 m with the glass mesh being 1.5×1.5 m, and the concentrated nodal mass is 146.25 kg (for a thickness of midhollow armored glass of 8 mm + 8 Air mm + 8 mm). The cable pretension $\overline{H_x}$ and $\overline{H_z}$ are 20 kN, the areas of the cables in the x and z directions are $202.3\text{E}-6\ \text{m}^2$, the Young's modulus of the cables is $1.3\text{E}11\ \text{N/m}^2$. The maximum central nodal displacement under the action of the mean wind load is 1/150 of the span of the cable net.

Eq. (21) is the Duffing equation, and in the undamped free vibration of Eq. (22), there is not only the harmonic component ω, but also 3ω, 5ω, and other high-order harmonic components by Kwan (2000). The preceding characteristic can be observed in the central nodal FEM time history displacement of the cable net, as shown in Fig. 4. However, the high-order harmonic components contribute a very small proportion and can be neglected. Fig. 5 shows that the larger the amplitude, the larger the nonlinear frequency.

The results from the three methods, given in Table 1, are very close. All of the errors are less than 0.9%. Thus, the analytical formula for the nonlinear frequency of Eq. (33) is considered to satisfy the precision requirement.

Nonlinear Elastic Single-Degree-of-Freedom Model

Figs. 3 and 6 show that the static and dynamic nonlinearity of cable net glazing needs to be considered, so the response spectrum method in the seismic design code by Ministry of Construction (2010) of China for linear and elastic structures has some limitations for the seismic design of nonlinear cable net glazing, and the geometric nonlinear response spectra for cable net glazing must be studied. The results of the shaking table test by Feng et al. (2009) showed that the first mode is dominant in the seismic displacement response of cable net glazing subject to seismic loads. Thus, the geometric nonlinearity of the structure is reflected in the first mode of cable net glazing. Because other modes play smaller roles in the displacement response, the other modes are less nonlinear. Therefore, only the nonlinear seismic response spectra of the first mode need be addressed. The nonlinear elastic single-degree-of-freedom model and the response spectra studied in this paper refer to the nonlinear response spectra of the first mode of cable net glazing. The nonlinear elastic single-degree-of-freedom model needs to be determined first.

As shown in Eq. (21), the nonlinear part of the structural stiffness includes the structural displacement, so the structural stiffness is

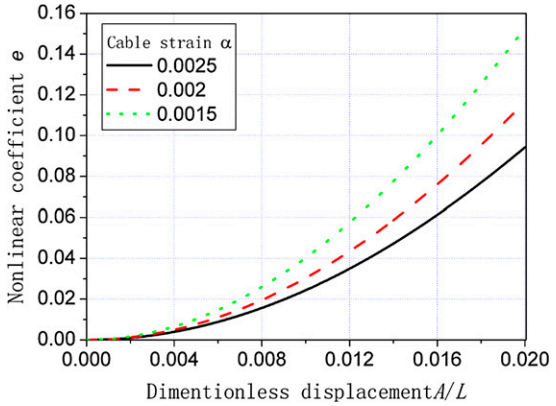

Fig. 4. Curves of the coefficient e of the nonlinear frequency versus amplitude-span ratios

J. Eng. Mech., 2013, 139(10): 1446-1459

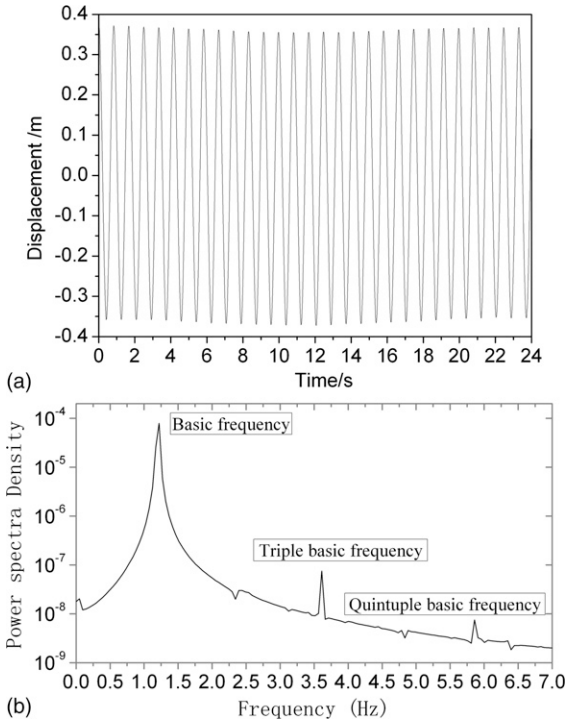

Fig. 5. Undamped free vibrating central displacement; (a) undamped free vibrating central time-history displacement; (b) power spectra density of central displacement

Table 1. Comparison of the Nonlinear Frequency Results from the Integral Algorithm, Analytical Formula, and FEM Time History Methods

Amplitude/ span	FEM (Hz)	Eq. (29) (Hz)	Error (%)	Analytical Eq. (32) (Hz)	Error (%)
0	1.0085	1.0127	0.411	1.0127	0.416
1/400	1.0104	1.015	0.45	1.015	0.45
1/200	1.0169	1.0218	0.48	1.0218	0.48
1/100	1.0421	1.0485	0.61	1.0485	0.61
1/50	1.1402	1.1483	0.71	1.1492	0.79
1/40	1.2083	1.2173	0.744	1.2189	0.877
1/30	1.3464	1.3535	0.53	1.3568	0.772

concerned with the structural displacement and hardened system. The multiple degrees of freedom of cable net glazing can be simplified to the nonlinear elastic single-degree-of-freedom system, as shown in Fig. 7.

The structural linear frequency in the vertical position is

$$\omega_1 = k_1/m = \left(\frac{\pi^2\overline{H_x}}{L_x^2} + \frac{\pi^2\overline{H_y}}{L_y^2}\right) \Big/ m$$

When the amplitude is A, the nonlinear frequency ω is given by Eq. (33).

When the linear frequency is ω_1, the linear natural period is T_l. When the nonlinear frequency is ω, the nonlinear natural period is T. Thus, the relationships among these parameters are

$$T_l = \frac{1}{\omega_l}, \quad T = \frac{1}{\omega}, \quad \omega_l < \omega,\ T_l > T$$

where $T = \mu T_l$, $\mu < 1$, and S'_a, S'_a, $S_a(T)$, and $S_d(T)$ are the absolute acceleration spectra and relative displacement spectra of the nonlinear and linear single-degree-of-freedom systems, respectively. Because the first natural period of cable net glazing is larger than 0.1 s, the relationship between the nonlinear and linear response spectra is

$$S'_a(T) = S_a(T_1) = S_a(\mu T_1) \geq S_a(T_1) \tag{35}$$

$$S'_d(T) = S_d(T_1) = S_d(\mu T_1) \geq S_d(T_1) \tag{36}$$

As shown in Eqs. (35) and (36), there may be a large difference between the response spectra of the linear and nonlinear single-degree-of-freedom systems. Design response spectra in the Chinese code for seismic design are given in Fig. 8, where the horizontal axis is the structural natural period, and the vertical axis is the structural absolute acceleration response. SI, SII, SIII, and SIV are four types of local site conditions. As shown in Fig. 8, when $\mu < 1$, for the response spectra of cable net glazing, the nonlinear response spectra can be regarded as the rightward movement of the linear response spectra because cable net glazing is a stiffness-hardening structure; therefore, the real working natural period of cable net glazing is less than the initial calculation period. While the period used in calculating the response spectra was the initial period, the real response spectra are the rightward movement of the calculating response spectra; that is, the response spectra move toward the long period.

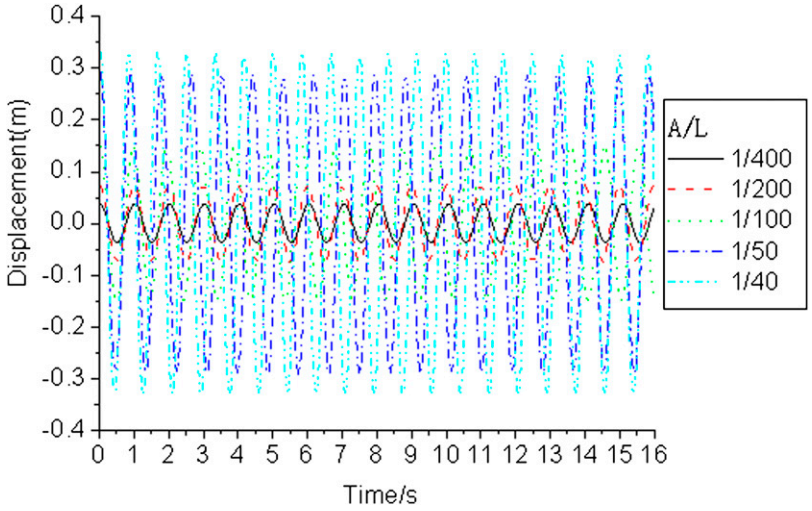

Fig. 6. Undamped free vibrating central nodal displacement of the cable net with different amplitudes

J. Eng. Mech., 2013, 139(10): 1446-1459

As the response spectra of the nonlinear single-degree-of-freedom system are different than those of the linear single-degree-of-freedom system, the linear response spectra in the seismic design code have some limitations for the seismic design of cable net glazing. The vibration displacement of cable net glazing changes during an earthquake, so the frequencies of cable net glazing also change, and it is very difficult to directly calculate the nonlinear response spectra of cable net glazing according to the nonlinear frequencies. The nonlinear response spectra can be determined only by the nonlinear single-degree-of-freedom model. Hence, the time history method was used to calculate the nonlinear response spectra of cable net glazing subject to seismic loads, and the nonlinear response spectra were also compared with the linear response spectra with different seismic waves and ground motion acceleration amplitudes.

Verification of the Nonlinear Single-Degree-of-Freedom Model

Verification of the Nonlinear Single-Degree-of-Freedom Model

The nonlinear single-degree-of-freedom model is given in Eq. (20). To verify the accuracy of the assumptions associated with the nonlinear vibration equation based on continuous membrane theory as described earlier, the precise results of the finite element (FE) model with the nonlinear time history method subject to seismic loads were compared with those of the nonlinear single-degree-of-freedom model in this paper. The time history response of the nonlinear single-degree-of-freedom model can be calculated using a direct numerical time integration scheme such as Newmark's method. The corresponding program for calculating the response of the nonlinear single-degree-of-freedom model can be developed with the Matlab software.

The following five FE models of cable net glazing with typical spans and height-to-width aspect ratios were chosen: Model 1, 21×21 m; Model 2, 18×12 m; Model 3, 30×15 m; Model 4, 36×12 m; and Model 5, 42×10.5 m, with height-to-width aspect ratios of 1, 2/3, 0.5, 1/3, and 0.25, respectively. The glass mesh is 1.5×1.5 m. Because the structural mass and seismic loads are symmetric, the seismic responses of the models with height-to-width aspect ratios 1.5 and 2/3 are the same, as are those of the models with

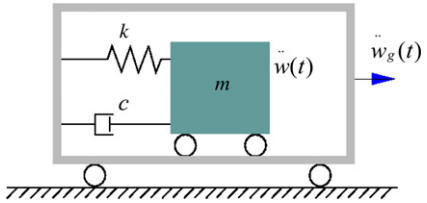

Fig. 7. Single-degree-of-freedom system

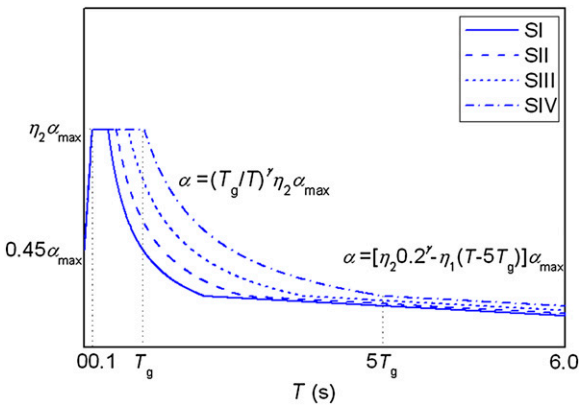

Fig. 8. Design response spectra in the Chinese code for seismic design

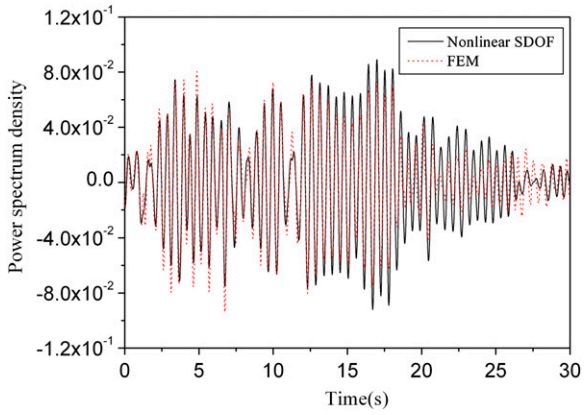

Fig. 9. Comparison of the time history curves for midpoint displacement for FE Model 1 and the nonlinear SDOF model

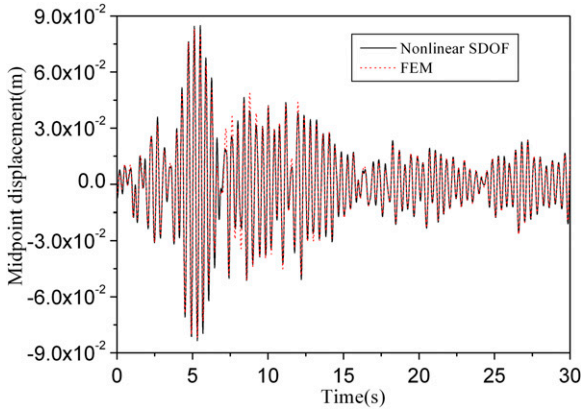

Fig. 10. Comparison of the time history curves for midpoint displacement for FE Model 2 and the nonlinear SDOF model

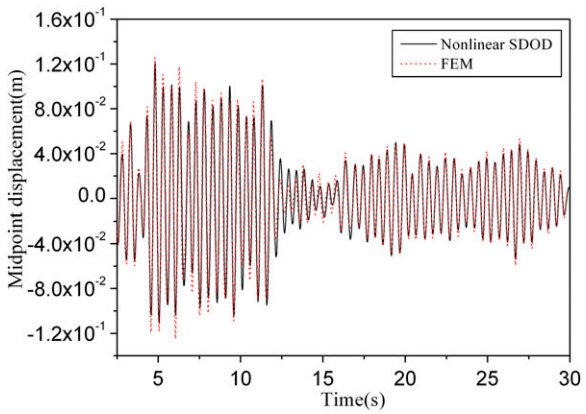

Fig. 11. Comparison of the time history curves for midpoint displacement for FE Model 3 and the nonlinear SDOF model

J. Eng. Mech., 2013, 139(10): 1446-1459

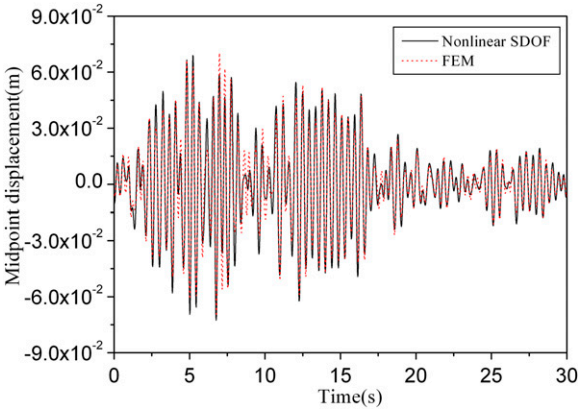

Fig. 12. Comparison of the time history curves for midpoint displacement for FE Model 4 and the nonlinear SDOF model

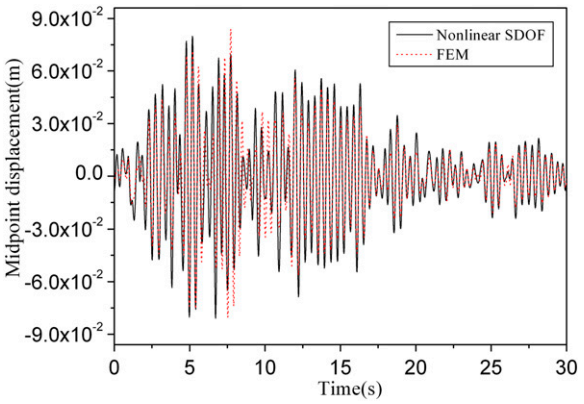

Fig. 13. Comparison of the time history curves for midpoint displacement for FE Model 5 and the nonlinear SDOF model

aspect ratios of 2 and 0.5, 3 and 1/3, and 4 and 0.25. Therefore, only the seismic responses of the models with height-to-width aspect ratios of 1, 2/3, 0.5, 1/3, and 0.25 are given. They are also the modes in Validity of the Nonlinear Single-Degree-of-Freedom Model and Verification of the Mode Decomposition Response Spectrum Method. The seismic design site condition modeled was Beijing on Site 1 in Group 1, and the earthquake action modeled was a rare 8-degree intensity earthquake. Earthquakes are described as 7, 8, and 9 degrees, and the degrees do not refer to Richter scale. The degrees are used to describe earthquake intensity in China code for seismic design of buildings, and the corresponding amplitude of the ground accelerations were 220, 400, and 620 gal, respectively. The predominant period of the site during the earthquake was 0.35 s.

Comparison of the time history curves of the midpoint displacement of the cable net glazing subject to a Taft wave with an acceleration amplitude of 400 gal, from the FE models and the nonlinear single-degree-of-freedom model, are shown in Figs. 9–13.

As Figs. 9–13 show, the time history curves of midpoint displacement from the five FE models and the nonlinear single-degree-of-freedom model are in most respects quite similar, and the largest displacements are nearly the same. The differences between the results from the FE models and the nonlinear single-degree-of-freedom model are due to the effect of the high modes of the cable net glazing. Thus, the assumptions associated with the nonlinear vibration equation based on continuous membrane theory and the

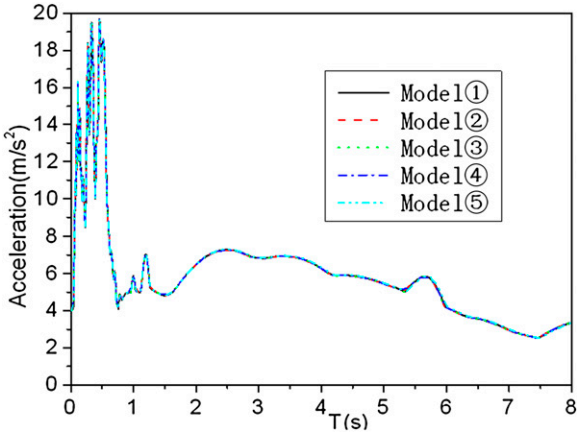

Fig. 14. Nonlinear acceleration response spectra of all models subject to an Olympia wave with 400 gal

nonlinear single-degree-of-freedom model presented in this paper is believed to be accurate.

Validity of the Nonlinear Single-Degree-of-Freedom Model

To validate the nonlinear single-degree-of-freedom model for cable net glazing, the acceleration spectra of cable net glazing, for the five models described earlier, were subjected to an Olympia (1949) wave with an acceleration amplitude of 400 gal. The geometric nonlinearity of the five models was the same. The acceleration spectra obtained for the five models are shown in Fig. 14. The acceleration spectra curves for all of the FE models are coincident, which indicates that the nonlinear single-degree-of-freedom model is reasonable. The nonlinear response spectra are connected only with the structural geometric nonlinearity of cable net glazing and have nothing to do with the spans and the height-to-width aspect ratios. Model 1 was used to calculate the response spectra of cable net glazing subject to seismic waves.

Nonlinear Spectra of Cable Net Glazing

El Centro and Olympia (1949) seismic waves were selected to calculate the response spectra of the nonlinear single-degree-of-freedom model, and all of the earthquake records were recorded on free fields or in the first floors of low-rise buildings.

The cable section and pretension of cable net glazing in the examples were determined by wind loads, and the frequencies were changed by the structural mass. The damping ratio of cable net glazing is not given in the seismic design code and glass curtain specification. On the basis of test results, the damping ratio was set at 0.02 in the examples by Feng et al. (2009). Because cable net glazing is a geometrically nonlinear structure, the nonlinearity of cable net glazing is closely related to its displacement, so both the acceleration response spectra and displacement response spectra are discussed in this paper. To compare the nonlinear and linear response spectra over a wide range of frequencies, the structural natural period was extended to 10 s, which is longer than the long limitation period in the Chinese code for the seismic design of buildings.

Comparisons of the nonlinear and linear response spectra for the Olympia (1949) and El Centro seismic waves are shown in

J. Eng. Mech., 2013, 139(10): 1446-1459

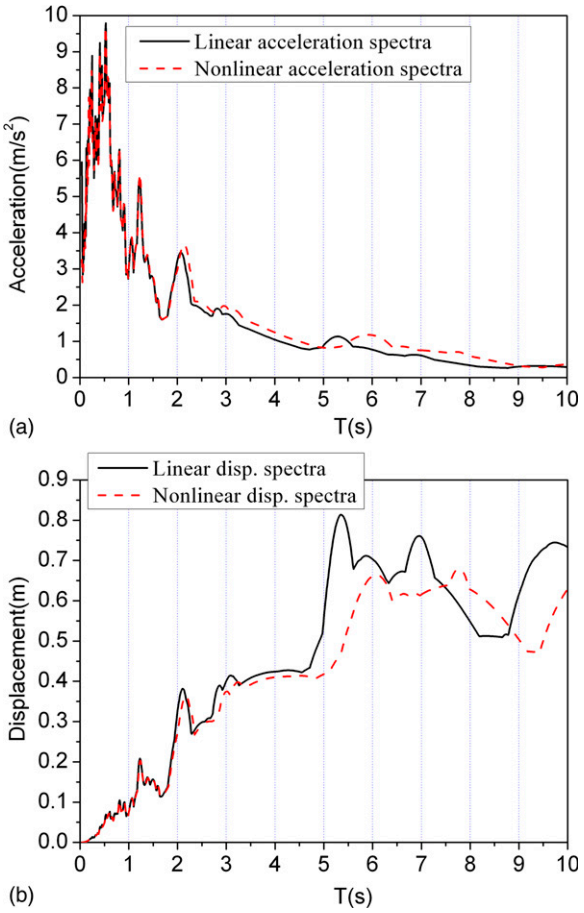

Fig. 15. Comparison of nonlinear and linear acceleration and displacement response spectra subject to an Olympia wave with 220 gal; (a) comparison of nonlinear and linear acceleration response spectra; (b) comparison of nonlinear and linear displacement response spectra

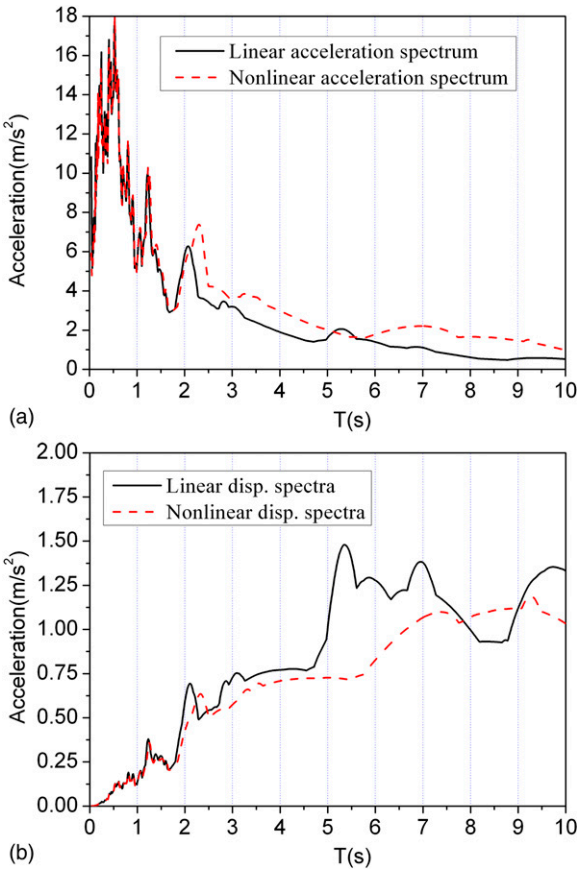

Fig. 16. Comparison of nonlinear and linear acceleration and displacement response spectra subject to an Olympia wave with 400 gal; (a) comparison of nonlinear and linear acceleration response spectra; (b) comparison of nonlinear and linear displacement response spectra

Figs. 15–20. The acceleration amplitudes of the seismic waves are 220, 400, and 620 gal, respectively, corresponding to rare earthquakes of 7, 8, and 9 degrees, respectively.

As shown in Figs. 15–20, when the natural period of cable net glazing is less than 2 s, the differences between the nonlinear and linear acceleration spectra are small. When the natural period of cable net glazing is larger than 2 s, which increases the natural period, the displacement of cable net glazing is larger than 1/50 of the structural span, and the nonlinear acceleration spectra are much larger than the linear acceleration spectra. The differences between the linear and nonlinear acceleration spectra are far smaller than those between the linear and nonlinear displacement spectra. The nonlinear period decreases as the structural displacement increases, so the nonlinear response spectra shape moves to the right compared with the linear response spectra shape. When the amplitudes of seismic waves are larger, the rightward movement of the response spectra is more obvious.

On the basis of comparisons between the nonlinear and linear response spectra for the three ground motion records analyzed, the conclusion can be drawn that when the natural period of cable net glazing is less than 2 s, the differences between the nonlinear and linear response spectra are small. This conclusion is very important because the first natural period of cable net glazing in practice is always less than 2 s. Thus, this conclusion is meaningful in a broader sense. The linear response spectra in the code for the seismic design of buildings can be used in the seismic design of cable net glazing as an approximation rather than the nonlinear response spectra of cable net glazing.

Dominant Modes in the Mode Decomposition Response Spectrum Method

Cable net glazing is a structure with multiple degrees of freedom, and when the mode decomposition response spectrum method is used in the seismic design of cable net glazing, there may be more than one mode that contributes to the seismic response. The number of modes that should be chosen, and which mode should be chosen, requires a criterion for choosing the dominant modes.

Criteria for Choosing Dominant Modes

For structures subject to dynamic loads, whether a mode is dominant or not depends on two important factors. First, the frequency of the mode should be included in the load frequency spectra; thus, the mode can be excited, and the closer the mode frequency is to the predominant frequency of dynamic loads, the greater the contribution of the mode is to the structural seismic response. Second, the relationship between the spatial distribution of dynamic loads and the vibration mode shape is very important, and the closer the spatial

J. Eng. Mech., 2013, 139(10): 1446-1459

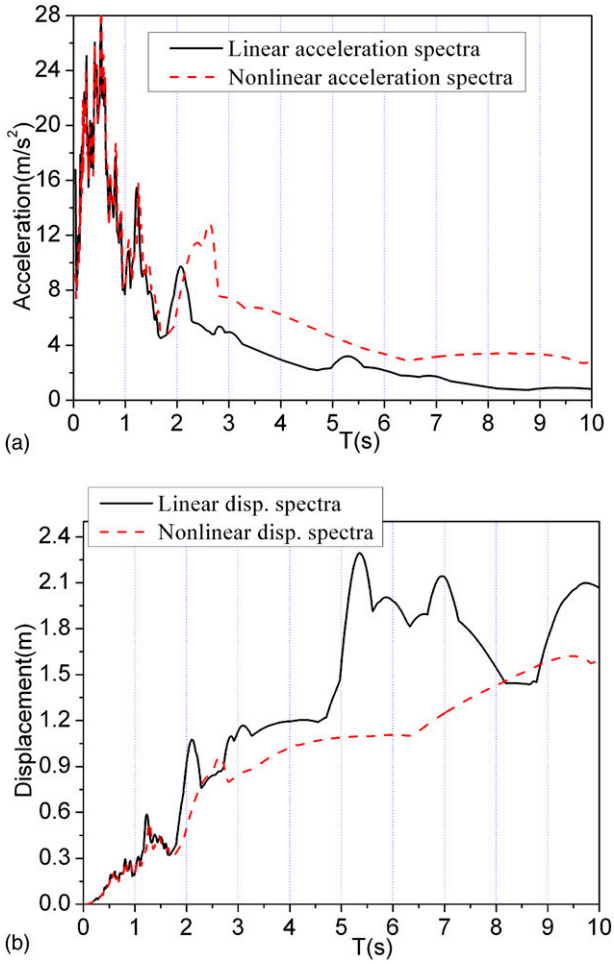

Fig. 17. Comparison of nonlinear and linear acceleration and displacement response spectra subject to an Olympia wave with 620 gal; (a) comparison of nonlinear and linear acceleration response spectra; (b) comparison of nonlinear and linear displacement response spectra

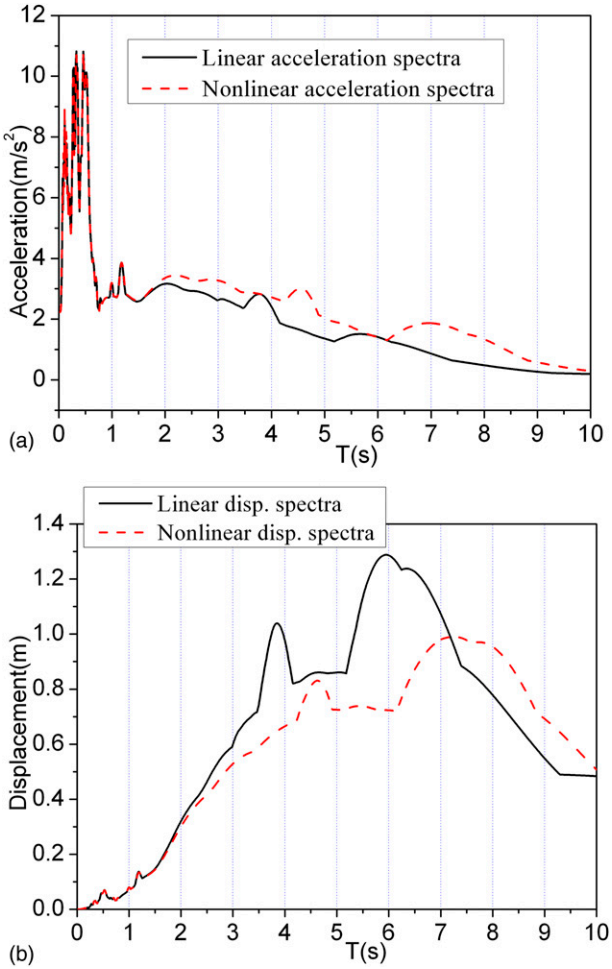

Fig. 18. Comparison of nonlinear and linear acceleration and displacement response spectra subject to an El Centro wave with 220 gal; (a) comparison of nonlinear and linear acceleration response spectra; (b) comparison of nonlinear and linear displacement response spectra

distribution of dynamic loads comes to the mode shape, the more easily the mode can be excited.

An earthquake wave is a narrow-band random process, and the frequencies of cable net glazing are within the range of the frequencies earthquake waves. The orthogonality between the spatial distribution of seismic loads and the vibration shape is the key factor in deciding whether the mode can be excited or not. The seismic load is $[M]\ \ddot{w}_g(t)$, $[M]$ is the structural mass matrix, and $\ddot{w}_g(t)$ is the ground motion acceleration. The mass matrix $[M]$ gives the spatial distribution of seismic loads, and the ground motion acceleration $\ddot{w}_g(t)$ gives the frequency content and intensity of the seismic load. Thus, the relationship between the spatial distribution of the seismic load and the vibration mode can be replaced by the relationship between the mass matrix $[M]$ and the vibration mode shape by Wilson et al. (1982).

The modal contribution coefficient is introduced to describe the relationship between the mass matrix and the vibration mode shape of cable net glazing, and it is used to choose dominant modes. The spatial pattern of the dynamic load can be expressed as shown in Eq. (37) by Joo et al. (1989):

$$F(s) = \sum_{j=1}^{n} \varphi_j^T F(s) M \varphi_j \tag{37}$$

The spatial pattern of the seismic load is the mass matrix:

$$F(s) = M$$

The modal contribution coefficient h_j, shown in Eq. (38), is the contribution of mode j to the spatial pattern of the seismic load by Gu et al. (2000). It describes the participation content of modes in seismic responses:

$$h_j = \frac{F^T(s)\varphi_j^T F(s) M \varphi_j}{F^T(s)F(s)} = \frac{M^T \varphi_j^T M M \varphi_j}{M^T M} A \tag{38}$$

The sum of the modal contribution coefficients h_j is equal to one.

Combination of Modal Responses

In the Chinese seismic code, the combination of the modal responses in the response spectrum method is the square root of the sum of the squares of the model responses (SRSS). For cable net glazing, the modal nodal displacements and cable forces were combined by the SRSS method. The SRSS combination method is applicable when the structure is linear. When the structure is geometrically nonlinear, the applicability of the SRSS combination method must

J. Eng. Mech., 2013, 139(10): 1446-1459

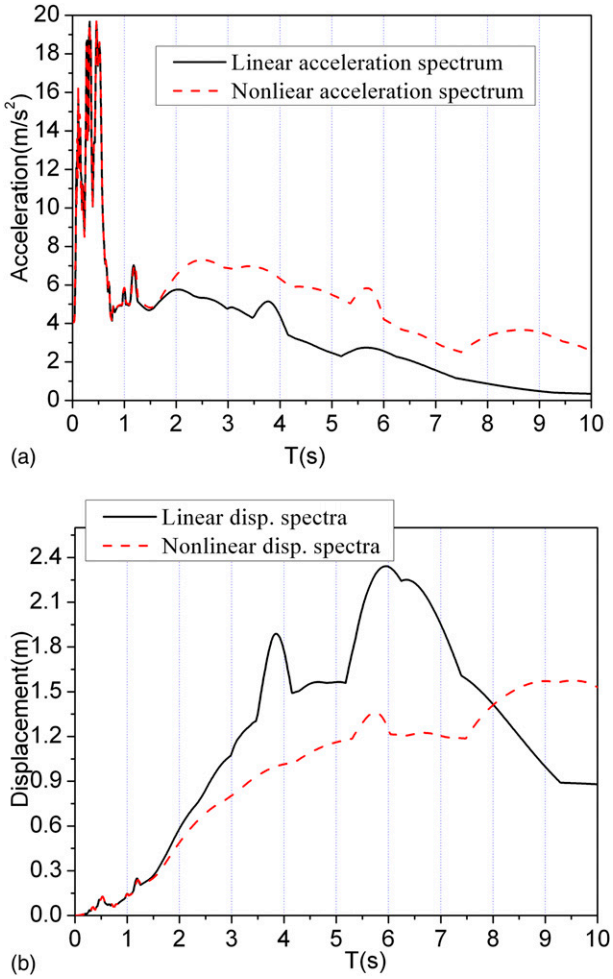

Fig. 19. Comparison of nonlinear and linear acceleration and displacement response spectra subject to an El Centro wave with 400 gal; (a) comparison of nonlinear and linear acceleration response spectra; (b) comparison of nonlinear and linear displacement response spectra

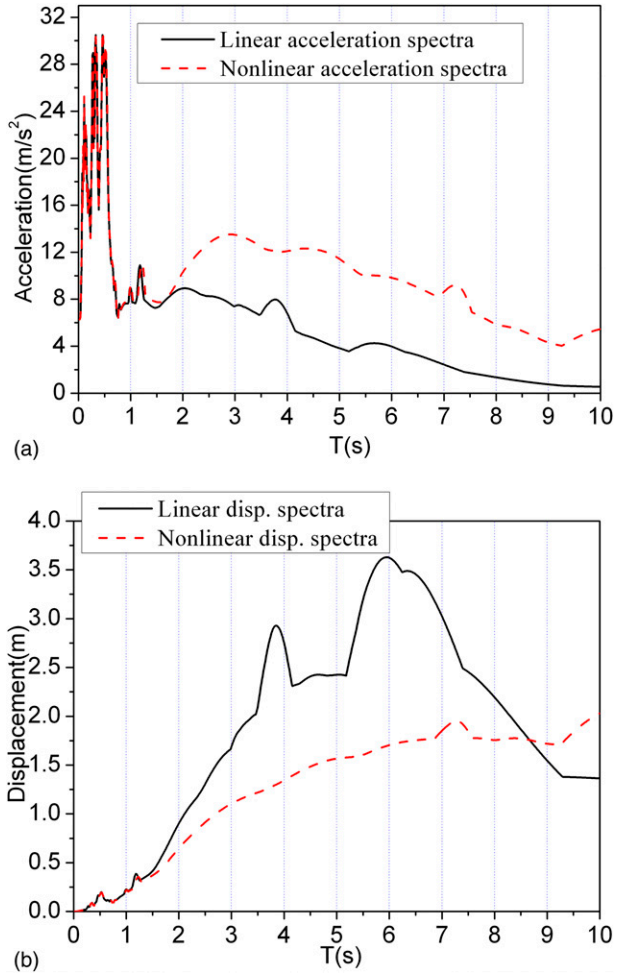

Fig. 20. Comparison of nonlinear and linear acceleration and displacement response spectra subject to an El Centro wave with 620 gal; (a) comparison of nonlinear and linear acceleration response spectra; (b) comparison of nonlinear and linear displacement response spectra

be considered. Every modal load was applied on cable net glazing, and a nonlinear static analysis was conducted. The load of all modes was applied on the structure simultaneously, and the cable net was modeled as a stiffness-hardening structure. The structural stiffness subject to every modal load is therefore less than the real structural stiffness subject to all modal loads. Thus, the structural seismic response with the SRSS combination is larger than the real seismic response of cable net glazing, and it is safer to use the SRSS combination. Feng et al. (2009) have shown that in the seismic response of cable net glazing, the first mode is dominant. Therefore, the error of the SRSS combination method might be small. The accuracy of the SRSS combination method was verified by the following nonlinear time history calculation with FE models.

Verification of the Mode Decomposition Response Spectrum Method

The five cable net glazing models described above were employed, and their seismic responses were calculated by the response spectrum method. The seismic design site condition was Beijing, on Site 1 in Group 1, and the earthquake action was a rare 8-degree intensity earthquake. The predominant period of the site during the earthquake was 0.35 s. The periods and mode shapes of the five FE models were computed using a commercial FE package, ANSYS.

The modal contribution coefficients of the first 30 modes of the five models are shown in Table 2. The proportional contribution of the first mode was more than 75% and played a major role. The modal contribution coefficients of symmetric modes are larger than those of asymmetric modes. Thus, the symmetric modes were the main modes in the vibration of the cable net under seismic loads, and the first mode was dominant.

The modal contribution to the structural displacement is shown in Figs. 22–26. The horizontal direction was assumed to be the x direction, the wind direction was the y direction, and the vertical direction was the z direction. The origin of the coordinates was the left corner of the cable net glazing. As the out-of-plane nodal displacements in the y direction were far larger than those in the x and z directions, which were in-plane nodal displacements, only the out-of-plane displacement in the y direction was compared. The nodal displacement along the vertical direction through the midpoint of the cable net glazing was chosen.

There are two hypotheses when the mode decomposition response spectrum method is used for cable net glazing. One is that the linear spectra can be substituted for the nonlinear spectra of cable net glazing. The other is that the structural stiffness subject to every modal load is

J. Eng. Mech., 2013, 139(10): 1446-1459

Table 2. Comparison of Maximum Cable Forces according to the Nonlinear Time History Method and Mode Decomposition Response Spectrum Methods

Mode participation coefficient	Mode 1	2	3	4	5	6	7	8	9	10	11	12	13	14	15
	16	17	18	19	20	21	22	23	24	25	26	27	28	29	30
Model 1	0.846	0.0	0.0	0.0	0.088	0.0	0.0	0.0	0.0	0.0	0.009	0.0	0.0	0.005	0.027
	0.0	0.0	0.0	0.0	0.0	0.0	0.003	0.0	0.0	0.0	0.0	0.0	0.0	0.0	0.0
Model 2	0.789	0.0	0.0	0.080	0.000	0.0	0.000	0.070	0.0	0.0	0.023	0.007	0.0	0.00	0.00
	0.000	0.0	0.0	0.000	0.008	0.0	0.014	0.000	0.0	0.0	0.000	0.000	0.001	0.000	0.000
Model 3	0.761	0.0	0.082	0.000	0.000	0.0	0.000	0.027	0.0	0.074	0.000	0.000	0.000	0.008	0.013
	0.000	0.0	0.000	0.003	0.000	0.0	0.000	0.000	0.0	0.00	0.000	0.006	0.001	0.000	0.019
Model 4	0.761	0.0	0.083	0.000	0.028	0.0	0.000	0.000	0.0	0.00	0.013	0.000	0.000	0.000	0.067
	0.000	0.0	0.009	0.006	0.000	0.0	0.000	0.003	0.0	0.000	0.004	0.001	0.000	0.000	0.000
Model 5	0.767	0.0	0.084	0.000	0.029	0.0	0.000	0.014	0.0	0.000	0.000	0.000	0.000	0.008	0.000
	0.000	0.0	0.000	0.005	0.063	0.0	0.007	0.000	0.0	0.000	0.002	0.000	0.003	0.000	0.000

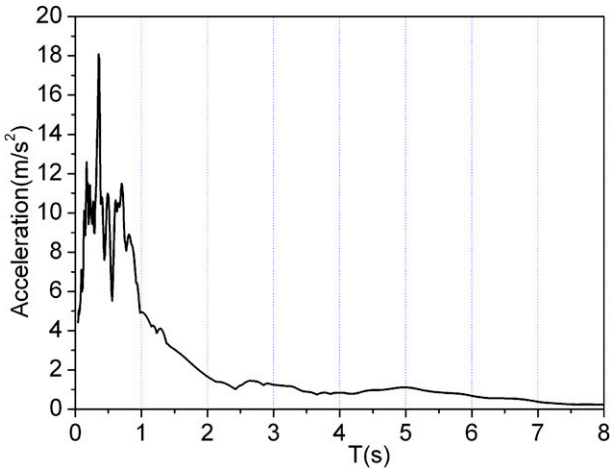

Fig. 21. Nonlinear acceleration response spectra subject to a Taft wave with 400 gal

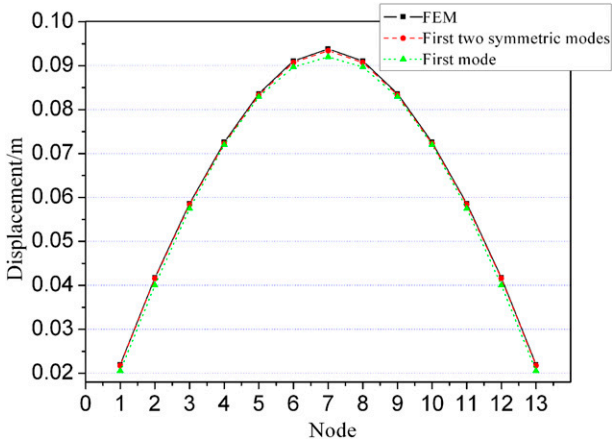

Fig. 22. Comparison of displacement of Model 1

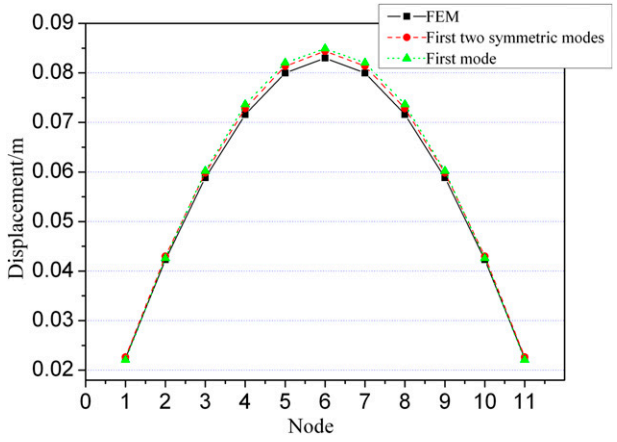

Fig. 23. Comparison of displacement of Model 2

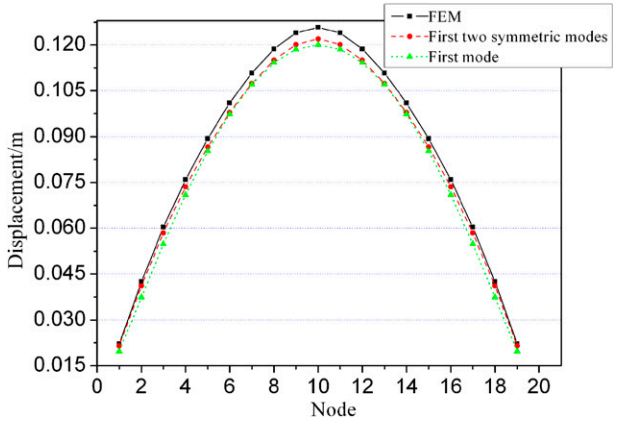

Fig. 24. Comparison of displacement of Model 3

less than the real structural stiffness subject to all modal loads and that the structural seismic response with SRSS combination is larger than the real seismic response of cable net glazing. The seismic responses corresponding to these two hypotheses will deviate from the real seismic responses. Thus, a nonlinear time history FE model was used to verify the mode decomposition response spectrum method.

When the mode decomposition response spectrum method was used to calculate the seismic response of the five models, the corresponding acceleration response spectra subject to different seismic waves were used. The acceleration response spectra subject to a Taft wave with 400 gal are shown in Fig. 21. Two types of combinations of modes were used. In combination 1, only the first mode was considered. Combination 2 considered only the first two symmetric modes.

Comparisons of displacements from the nonlinear time history analysis and the mode decomposition response spectrum method

J. Eng. Mech., 2013, 139(10): 1446-1459

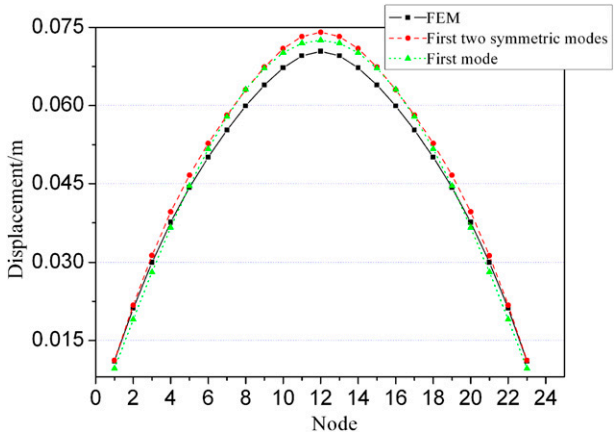

Fig. 25. Comparison of displacement of Model 4

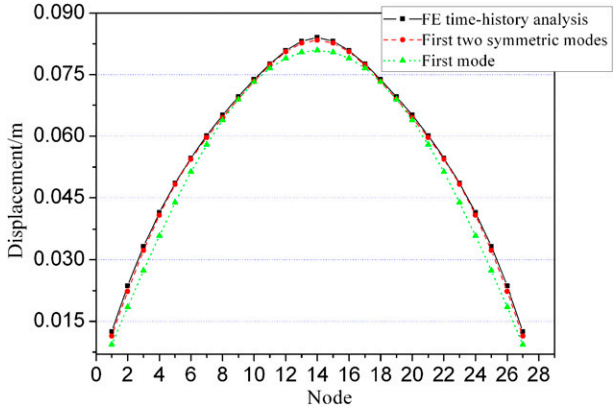

Fig. 26. Comparison of displacement of Model 5

Table 3. Comparison of Maximum Cable Forces According to the Nonlinear Time History Method and Mode Decomposition Response Spectrum Methods

Maximum cable tension (kN)	Model 1	Model 2	Model 3	Model 4	Model 5
First mode	4.774	6.911	11.758	6.750	8.833
First two symmetric modes	4.781	6.913	11.932	6.756	8.849
Time history analysis	4.834	6.916	12.141	6.757	8.850

subject to a Taft wave are shown in Figs. 22–26. The out-of-plane nodal displacement along the vertical direction through the midpoint of cable net glazing was chosen. As Figs. 22–26 show, the displacement errors were all less than 6%. As the height-to-width aspect ratio increased, the error of combination one increased. The error of the nodal displacement at the edge of the cable net glazing was far larger than the error of the midpoint displacement. When the height-to-width aspect ratio was equal to 0.5, the displacement error was less than 11%. When the height-to-width aspect ratio was equal to 0.25, the error of the nodal displacement at the edge of the cable net glazing was 27%, which indicates that the higher-order modes play a role in the structural seismic response. The error of the nodal displacement at the edge of the cable net glazing in combination 2 was less than 10%.

The maximum cable forces for the five models by the three methods are given in Table 3. The pretension in the cable forces was excluded. As shown in Table 3, the differences in the cable forces in the three methods for the five models were small. As shown in Eqs. 4–5, the increase in the cable force is proportional to the increase in the square of the displacement derivative. When the rotation angle (equivalent to the displacement derivative) of the cable net that is caused by the displacement is very small, the variation amplitude of the cable tension is far less than that of the displacement.

Based on the analysis of the seismic responses of the five models by the three methods, the following conclusions can be drawn. The mode decomposition response spectrum method is applicable to calculation of the seismic response of cable net glazing, and the first mode is dominant in the seismic response of cable net glazing. When the height-to-width aspect ratio is between 0.5 and 2, the first mode is sufficient for calculation of the seismic response of cable net glazing. When the height-to-width aspect ratio is not between 0.5 and 2, the first mode is accurate only in the largest displacement. If all the responses of the cable net glazing are needed, the modal contribution coefficient can be used to choose the dominant modes for cable net glazing precisely. Use of the first two symmetric modes is an approximate method.

Conclusions

1. The continuous membrane theory is used to construct the static equilibrium equation and the nonlinear vibration differential equation of cable net glazing subject to earthquakes, and the harmonic balance method is used to solve the analytic formula of the nonlinear frequency. The analytic formula of the nonlinear frequency is simple, highly precise, and convenient for use in engineering practice. The static and dynamic geometric nonlinearity of cable net glazing is discussed in detail.
2. The nonlinear vibration differential equation and nonlinear frequency presented in this paper form the basis of the nonlinear single-degree-of-freedom model for cable net glazing. The nonlinear response spectra were determined using the nonlinear single-degree-of-freedom model.
3. The nonlinear natural period decreases as the structural displacement increases. Thus, the nonlinear response spectra shape moves to the right compared with the linear response spectra shape. When the amplitudes of the seismic waves are larger, the rightward movement of the response spectra is more obvious.
4. Because the first natural period of cable net glazing is always less than 2 s in practice, the linear response spectra in the code for the seismic design of buildings can be used in the seismic design of cable net glazing as a reasonable approximation, in place of the nonlinear response spectra of cable net glazing.

Acknowledgments

This research was financially supported by the Natural Science Foundation of China under Grant Nos. 50908044, 51278117, and 51125031, State Key Laboratory of Subtropical Building Science of South China University of Technology under Grant No. 2011KA05, Jiang Su provincial Natural Science Foundation of China under Grant No. SBK201123270, and a project funded by the Priority Academic Program Development of Jiangsu Higher Education Institutions.

References

Brodniansky, J., and Aroch, R. (2001). "Glass and steel structure." *Proc., International Symp. on Theory, Design and Realization of Shell and Spatial Structures*, Architectural Institute of Japan, Tokyo.

Dechao, Z., and Yufeng, X. (2004). *Base of engineering vibration*, Beijing Univ. of Aeronautics and Astronautics Press, Beijing.
Feng, R. Q., Wu, Y., and Shen, S. Z. (2007). "Working mechanism of single-layer cable net supported glass curtain walls." *Int. J. Adv. Struct. Eng.*, 10(2), 183–195.
Feng, R. Q., Yao, B., Wu, Y., and Shen, S. Z. (2010). "Dynamic performance of cable net glazing with consideration of glass panels under earthquake." *J. Harbin Inst. Tech.*, 17(3), 313–317.
Feng, R. Q., Ye, J. H., Wu, Y., and Shen, S. Z. (2012). "Mechanical behavior of glass panels supported by clamping joints in cable net facades." *Int. J. Steel Struct.*, 12(1), 15–24.
Feng, R. Q., Zhang, L. L., Wu, Y., and Shen, S. Z. (2009). "Dynamic performance of cable net glazing." *J. Constr. Steel Res.*, 65(12), 2217–2227.
Gu, J., Ma, Z.-D., and Hulbert, G. M. (2000). "A new load-dependent Ritz vector method for structural dynamics analyses: Quasi-static Ritz vectors." *Finite Elem. Anal. Des.*, 36(3–4), 261–278.
Irivne, H. M. (1992). *Cable structure*, Dover, New York.
Joo, K.-J., Wilson, E. L., and Leger, P. (1989). "Ritz vectors and generation criteria for mode superposition analysis." *Earthquake Eng. Struct. Dynam.*, 18(2), 149–167.
Krishna, P. (1978). *Cable-suspended roofs*, McGraw-Hill, New York.
Kwan, A. S. K. (2000). "A simple technique for calculating natural frequencies for geometrically nonlinear prestressed cable structure." *Comput. Struc.*, 74(1), 41–50.
Ministry of Construction. (2003). "Chinese technical code for glass curtain wall engineering." *JGJ102-2003*, Beijing.
Ministry of Construction. (2010). "Code for seismic design of buildings." *GB50011-2010*, Beijing.
Ministry of Construction. (2012). "Technical specification for cable structures." *JGJ257-2012,* Beijing.
Nayfeh, A., and Mook, D. T. (1979). *Nonlinear oscillations*, Wiley-Interscience, New York.
Pantelides, C. P., Trueman, K. Z., and Beha, R. A. (1996). "Development of a loading history for seismic testing of architectural glass in a shop-front wall system." *Eng. Struct.*, 18(12), 917–935.
Saitoh, M., Okada, A., and Imamura, R. (2001.). "Study on glass supporting system pinched at corner structural characteristics and structural design method." *Proc., International Symp. on Theory, Design and Realization of Shell and Spatial Structures*, Architectural Institute of Japan, Tokyo.
Schlaich, J. (2004). "Conceptual design of light structures." *J. Int. Assoc. Shell Spatial Struct.*, 45(1), 157–168.
Schlaich, J., Schober, H., and Moschner, T. (2005). "Prestressed cable net glazing." *Struct. Eng. Int.*, 15(1), 36–39.
Schober, H., and Scheider, J. (2004). "Developments in structural glass and glass structures." *Struct. Eng. Int.*, 14(2), 84–86.
Vyzantiadou, M. A., and Avdelas, A. V. (2004). "Point fixed glazing systems: Technological and morphological aspects." *J. Constr. Steel R.*, 60(8), 1227–1240.
Wilson, E. L., Yuan, M. W., and Dickens, J. M. (1982). "Dynamic analysis by direct superposition of Ritz vectors." *Earthquake Eng. Struct. Dynam.*, 10(6), 813–821.